Third International Conference on Sustainable Construction Materials and Technologies http://www.claisse.info/Proceedings.htm

# An Effective Way to Incorporate Nano-$TiO_2$ in Photocatalytic Cementitious Materials

Ming Zhi Guo, Chi Sun Poon*

**Department of Civil and Environmental Engineering*
*The Hong Kong Polytechnic University,*
*Hung Hom, Kowloon, Hong Kong*
*E-mail: cecspoon@polyu.edu.hk*

## ABSTRACT

In this study, a spraying method was employed to coat nano-$TiO_2$ particles on the surface of concrete surface layers. For comparison reasons, an intermixing method was also used to embed 5% nano-$TiO_2$ particles in the testing samples. Photocatalytic degradation of NO was evaluated to compare their air-purifying efficiencies. A harsh abrasion was imposed on the testing samples to evaluate the resistance of the surface $TiO_2$-particles to weathering. The results showed that after 7 days curing, all the $TiO_2$ sprayed samples displayed higher photocatalytic NO removal activities than the $TiO_2$ intermixed samples. After 28 days curing, a slight reduction in NO removal was observed. Although abrasion exerted a significant photocatalytic reduction on the $TiO_2$ sprayed samples, they still retained a NO removal ability that was higher than that of the $TiO_2$ intermixed samples.

**Keywords:** Titanium dioxide; NO removal; Cementitious materials; Spraying; Weathering

## 1. INTRODUCTION

Combining photocatalysts (particularly $TiO_2$) with cementitious materials generates a range of functional photocatalytic concrete products (Chen and Poon, 2009). Properties such as self-cleaning (Diamanti et al., 2008; Rout et al., 2009; Chen et al., 2011), antimicrobial (Guo et al., 2012a) and air purification (Poon and Cheung, 2007; Ramirez et al., 2010) have been demonstrated. The most attractive is that the realization of these functions only needs natural solar energy as the energy source. Under irradiation of solar light, photons with energies equal to or higher than the band gap are absorbed by the photocatalyst. This absorbed energy enables the formation of subsequent reactive species with oxidation and reduction power, which ultimately carry out the photocatalytic activities (Fujishima et al., 2000; Fujishima et al., 2008; Henderson, 2011). This gives it a big advantage as an environmentally friendly way of tackling of plaguing environmental problems. Therefore, photocatalytic cementitious materials find favor with many researchers on a global scale.

Until now, the predominantly adopted $TiO_2$ adding method in the concrete products is by intermixing it into the cementitious matrix of various building materials. From a practical perspective, this is efficient as this method allows the embedded nano-$TiO_2$ particles protected by the cementitious materials and can withstand harsh and aggressive environments in which they are put into use. On the other hand, the cementitious materials can also benefit from the addition of nano-$TiO_2$ particles. For example, the compressive strength of nano-$TiO_2$ containing mortars was found to be higher than the samples without nano-$TiO_2$ particles (Guo et al., 2012). However, the intermixing method is cost-prohibitive due to the

requirement of incorporation of a large amount of $TiO_2$ particles. Moreover, another down side is that not all of the initially added $TiO_2$ particles in the resulting products could be fully utilized for the photocatalytic reaction, because the nano-$TiO_2$ particles may be encapsulated by the hydration cement products. As a consequence, a significant loss of the photocatalytic activity would be observed when the concrete ages. It has been found that cement mixtures containing $TiO_2$ were significantly less efficient than $TiO_2$ slurries in decomposing 3-nitrobenzenesulfonic (Rachel et al., 2002). It is thought that the reduction of active surface and the presence of ionic species, which contributed to the charge recombination, are the reasons for the catalytic activity loss.

To avoid the reduction in photocatalytic activity, the dip-coating method seems to be an attractive alternative. By coating nano-$TiO_2$ particles on the surface of the cementitious materials, not only a significantly higher photocatalytic activity can be expected, but a much lower $TiO_2$ dosage and hence cost is needed. Compared to 5% nano-$TiO_2$ intermixed mortars, mortars dip-coated with nano-$TiO_2$ solution displayed a highly improved photocatalytic activity as reflected by a total inactivation of bacteria (Guo et al., 2012b). But the dip-coated option suffers from a considerable loss in photocatalytic activity when they are exposed to harsh environmental conditions as the $TiO_2$ particles on the surface are prone abrasion and other form of deterioration conditions. For example, it was found that the $TiO_2$ dip-coated mortars almost completely lost their bacteria inactivation ability after undergoing an abrasion condition (Guo et al., 2012b). Moreover, the $TiO_2$ dip-coating technique for mortars would not be a practical from an industrial production perspective.

In this study, we try to find a simple and effective method to combine nano-$TiO_2$ in photocatalytic cementitious materials. By spraying the $TiO_2$ solution immediately on the surface of freshly prepared concrete surface layers, a high photocatalytic activity is expected. Also, the cost of $TiO_2$ is favorably reduced as only the surface contains $TiO_2$. However, this seemingly promising method would naturally raise a few reasonable questions: a) as the hydration proceeds, would the sprayed nano-$TiO_2$ particles be masked by the hydration products? b) whether the sprayed nano-$TiO_2$ particles can last after exposed to aggressive conditions?

## 2. EXPERIMENTAL STUDY

### *2.1. Materials and sample preparations*

In all the experiments, a commercially available nano-$TiO_2$ powder (P25, Degussa) was used as the photocatalyst. The particle size of the $TiO_2$ was 20-50 nm, with a specific BET surface area of 50 ±15 $m^2 g^{-1}$. ASTM Type I Ordinary Portland cement (OPC, Green Island Cement Limited, Hong Kong) and fly ash (FA) were used as the cementitious materials. In preparing the nano-$TiO_2$-based concrete surface layers, crushed recycled glasses (RG) derived from post-consumer beverage glass bottles were used as fine aggregates. The use of recycled glass cullets to produce decorative concrete provides a sustainable way to reuse and recycle the waste glass, easing the burden on the landfills. On the other hand, the light transmitting properties and different colours and varieties of glass cullet will make the resulting products more aesthetically pleasing. The post-consumer beverage glass used was sourced from a local eco-construction material company. Prior to the experimental use, all the discarded glass bottles were washed, sorted by colour and then crushed by a mechanical crusher, followed by sieving to a desired particle size. The characteristics of the recycled glass cullets (light green colour) used in the experiment are shown in Table 1.

**Table 1. Particle size distributions of glass**

| Sieve size (mm) | Recycled glass (% passing) |
|---|---|
| | Light green glass |
| 5.0 | 99.6 |
| 2.36 | 86.7 |
| 1.18 | 51.9 |
| 0.6 | 26.6 |
| 0.3 | 12.4 |
| 0.15 | 5.3 |

The mix proportion (by weight) for the concrete surface layers was 0.75:0.25:3.0:0.3 (OPC: FA: RG: water). To prepare the $TiO_2$-intermixed samples, a dosage of nano-$TiO_2$ (5% by cementitious materials weight) as an addition to the mixture was adopted. The surface layers were fabricated in steel moulds with an internal dimension of 200×100×5mm (Fig. 1). The procedures for the preparation of the concrete surface layers were as follows. First, all the proportioned materials were mixed uniformly for about 5 min using a mechanical mixer. For each concrete surface layer, 250 g well-mixed materials were weighted. Then, the steel moulds were over filled with the mixed materials and hand compacted, followed by being further compressed twice using a compression machine at a rate of 500 kN min, firstly to 500 kN and secondly to 600 kN. After one day, the surface layers were removed from their moulds and were tightly wrapped by plastic films for curing until testing.

**Figure 1. Steel mould (Internal dimension: 200×100× 5 mm)**

To prepare the $TiO_2$ sprayed samples, a suspension of methanol and P25 (25 g/L) was prepared. Three sets of $TiO_2$ sprayed specimens were prepared (Table. 2). The first set was prepared by spraying $TiO_2$ solution directly on the surface of the concrete surface layers 30 times after the mechanical compaction (Spray A). For the second set, the surface layers were first sprayed with the $TiO_2$-solution 15 times,

followed by mechanical compaction, and for another 15 times after the compaction (Spray AB). For the third set, the surface layers were sprayed with $TiO_2$-solution 30 times immediately after putting the materials into the steel mould and before applying the mechanical compaction (Spray B). All the spraying was performed within 10 min after the surface layers were prepared.

**Table 2. Three $TiO_2$-sprayed methods**

| Sample ID | Description |
|---|---|
| Spray A | Surface layers were sprayed with the $TiO_2$-solution 30 times after mechanical compacting |
| Spray AB | Surface layers were sprayed with the $TiO_2$-solution 15 times before compacting and another 15 times after compacting |
| Spray B | Surface layers were sprayed with the $TiO_2$-solution 30 times before compacting |

### *2.2. Weathering conditions for $TiO_2$-intermixed and $TiO_2$-sprayed samples*

To evaluate and compare the resistance of the $TiO_2$-intermixed and $TiO_2$-sprayed samples to weathering, a harsh abrasion was applied to the surface of the testing specimens. A concrete block with a dimension of 200×100×60mm which weighs 2850 g was used to apply the load. Figure 2 shows the used concrete block. The abrasion was applied by means of an abrasive paper (grade: Cw 220-2c) which was firmly attached on the surface of the block. The testing surface layer was first fixed by putting it into a steel mould. Then, the block with the abrasive paper was placed on the surface of the samples. The block with the attached abrasive paper was pushed back and forth from one end to the other end of the surface layer (no extra weight was added except the weight of the block). After every ten times of abrasion, the sample was taken to test for its change in photocatalytic activity.

**Figure 2. Concrete block used to apply the abrasion load**

### *2.3.Photocatalytic conversion of NO*

#### *2.3.1. Reactor setup*

The reactor was made according to the specifications of JIS R1701-1 with slight modifications. The dimension of the reactor was 700 mm in length, 400 mm in width and 130 mm in height (Fig. 3). Testing samples were placed on a rack at the centre of the reactor. Two UV-A fluorescent lamps (TL 8W/08 BLB, Philips, Holland) were positioned parallel to each other on the glass cover of the reactor to provide UV radiation. The wavelength of the lamps ranged from 300 to 400 nm with a maximum intensity of 365 nm. The UV between the lamps and the reactor could be adjusted to achieve a required intensity. The UV intensity was measured by a digital radiometer equipped with a DIX-365A UV-A sensor (Spectroline DRC-100X, spectronics corporation, USA). A zero air generator (Thermo Environmental Inc. Model 111) was used to supply a constant clean air flow. The testing gas was a mixture of zero air and standard NO (Arkonic Gases, Hong Kong). The humidity in the reactor was controlled by passing the zero air stream through a humidification chamber. The NO concentration was continuously measured using a Chemilluminescence NO analyzer (Thermo Environmental Instruments Inc. Model 42c, USA). A thermometer, a humidity sensor and an adjustable rack supporting the specimens were placed inside the reactor. The reactor was completely sealed with no detectable leakage.

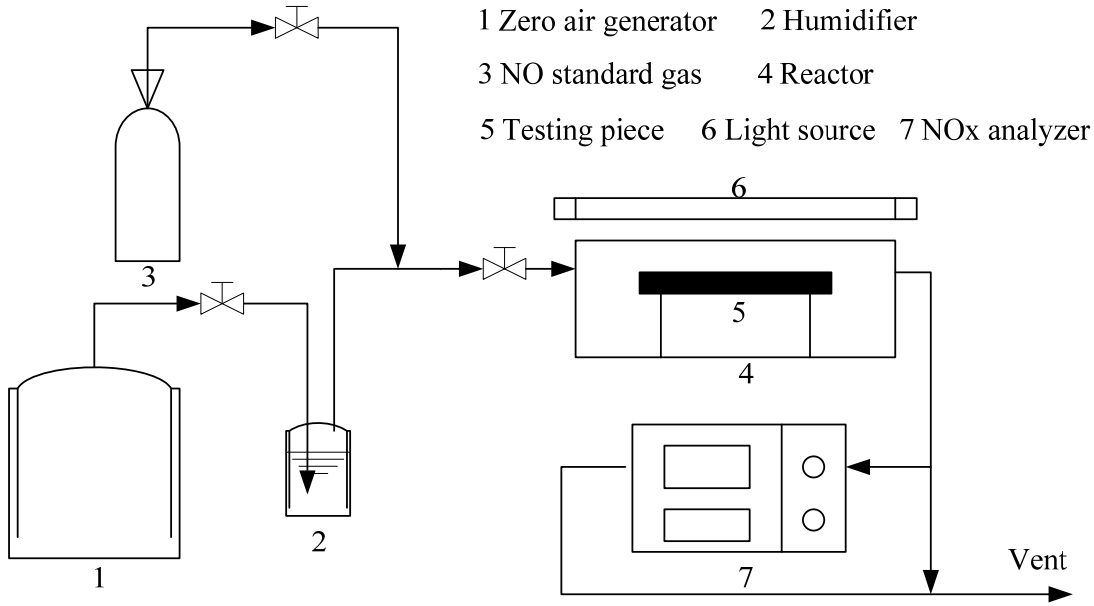


**Figure 3. Schematic diagram of NO removal experimental set-up**

#### *2.3.2. Testing protocol*

All the experiments were carried out at the ambient temperature (25±3℃). The flow of the testing gas (1000 ppb NO) was adjusted by two flow controllers to a rate of 3 L $min^{-1}$ and the relative humidity (RH) was controlled at 50±5%. The UV intensity was 10 $Wm^{-2}$ at the centre of the reactor. Prior to all photocatalytic conversion processes, the testing gas stream was introduced to the reactor in the absence of UV radiation for at least half an hour to obtain a desired RH as well as gas-solid adsorption-desorption equilibrium. Then the UV lamps were turned on for the photocatalysis process to begin. For each sample

the NO removal test lasted for 1 h and the concentration change of NO and $NO_2$ at the outlet was recorded. Due to the small amount of $NO_2$ generation (less than 30 ppb in all tests), the photocatalytic ability of the samples was expressed by NO reduction. Every sample was tested three times and the average value together with the standard deviation was reported. The calculation of the amount of NO removal, following the instructions in JIS R 1701-1, is shown below:

$$Q_{NO} = \left(\frac{f}{22.4}\right) \cdot \int ([NO]_0 - [NO])\, dt \quad (1)$$

where:

$Q_{NO}$: the amount of nitrogen monoxide removed by the test sample (μmol)

$[NO]_0$: inlet concentration of nitrogen monoxide (ppm)

[NO]: outlet concentration of nitrogen monoxide (ppm)

t: time of removal operation (min)

*f*: flow rate converted into that at the standard state (0℃, 1.013 kPa) (L $min^{-1}$)

The specific NO removal in units of mg $h^{-1}$ $m^{-2}$ is calculated by the following formula:

$$\theta = \frac{Q_{NO} \times MW_{NO} \times 10^3}{\text{Sampling time (h)} \times \text{Surface area } (m^2)} \quad (2)$$

where:

θ: specific photoactivity (mg $h^{-1}$ $m^{-2}$)

$Q_{NO}$: the amount of nitrogen monoxide removed by the test sample (mol)

$MW_{NO}$: the molecular weight of NO

## 3. RESULTS and DISCUSSION

### *3.1. Effects of different methods and curing age on NO photodegradation*

The photocatalytic NO removal performance of the different samples at different curing ages (7 days and 28 days) is shown in Fig. 4. For the reference samples (without the addition of $TiO_2$), there was negligible NO removal observed after both 7 and 28 days curing. After 7 days curing, the 5% $TiO_2$-intermixed samples exhibited an approximately 4 mg $h^{-1}$ $m^{-2}$ NO removal on average. In contrast, all the $TiO_2$-sprayed samples showed a significantly higher NO removal ability. Among the $TiO_2$-sprayed samples, Spray A and Spray AB had similar NO removal rates, 6.31 and 6.38 mg $h^{-1}$ $m^{-2}$ respectively. On the other hand, Spray B displayed a lower NO removal rate of 5.45 mg $h^{-1}$ $m^{-2}$. It is likely that the compression made the $TiO_2$ more intimately combined with the cementitious materials, and some particles thus lost their photocatalyic activity. The comparison between $TiO_2$-intermixed samples and $TiO_2$-sprayed samples clearly demonstrates that by spraying the $TiO_2$ particle on the surface of the cementitious substrate, the flowing NO gas had more extensive and convenient contact with the active $TiO_2$ sites.

Compared to that at 7 days curing age, except for the Spray A samples, all the other samples experienced a loss in photocatalytic NO removal activity at 28 days curing age. The reduction was more evident for the 5% $TiO_2$-intermixed samples, whereas, Spray AB and Spray B only suffered a slight loss. It seems that as the hydration proceeded, $TiO_2$ particles which were closely surrounded by the cementitious materials had a higher chance to firmly combine with the hydration products. As a result, the hydration products blocked the access of NO gas to the $TiO_2$ activate surface, thus a drop in NO removal rate.

Another advantage of the spraying method is its lower cost. By rough calculation, 2.2g of $TiO_2$ particles is required for one piece of 250g 5% $TiO_2$-intermixed surface layer. In contrast, for one piece of 30 times $TiO_2$-sprayed surface layers, only 0.62g of $TiO_2$ particles are needed.

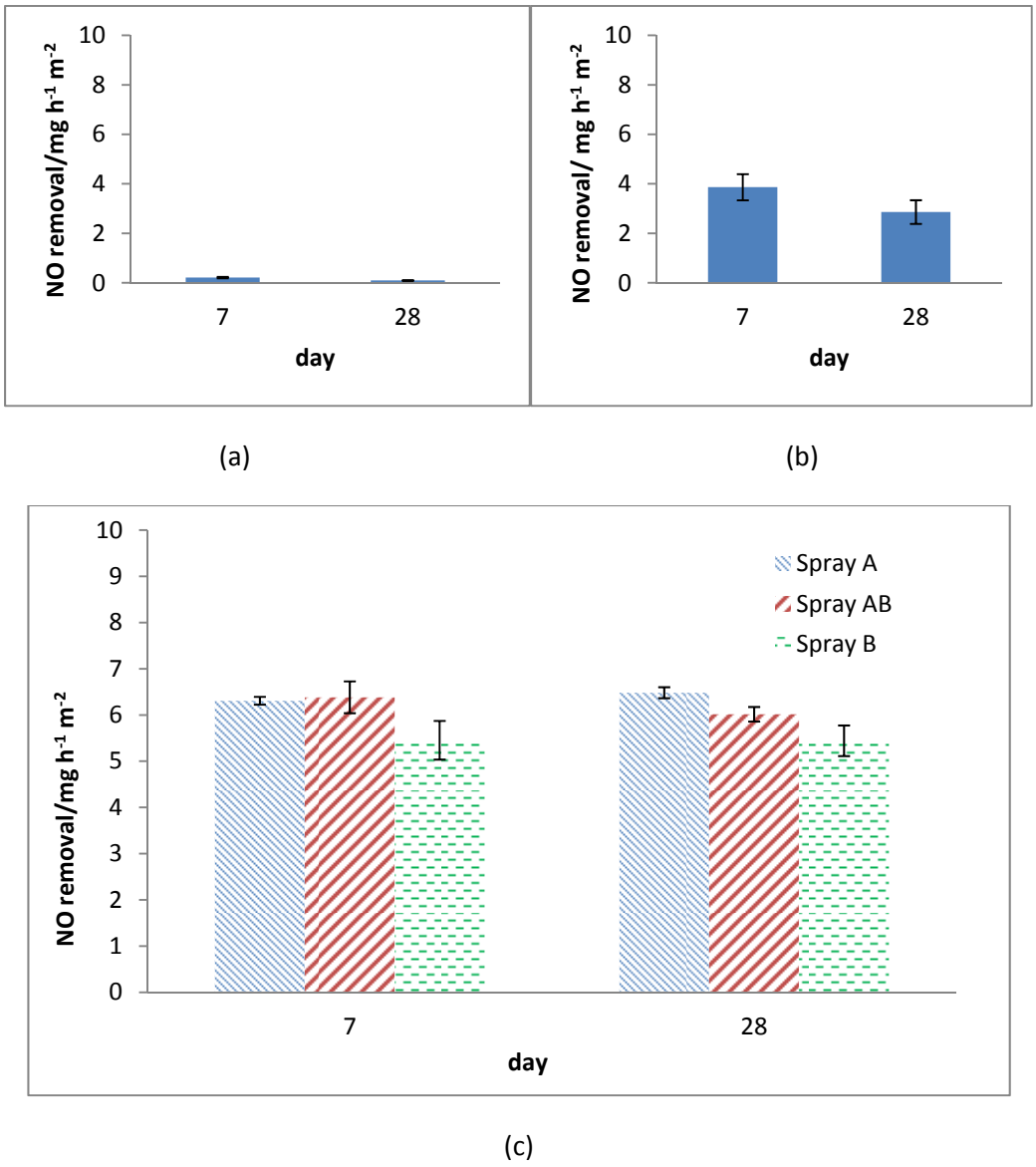


**Figure 4. Photocatalytic NO removal performance of different samples: (a) Reference without $TiO_2$), (b) 5%$TiO_2$-intermixed, (c) $TiO_2$-Sprayed Samples**

### *3.2. Effects of abrasion on NO photodegradation of $TiO_2$-intermixed and $TiO_2$-sprayed samples*

To evaluate the tolerance of the different samples to abrasion (weathering), the abrasion condition described above was applied to the surface of the testing samples. Given its high NO removal efficiency (similar to that of Spray A and higher than that of Spray B), coupled with the fact that mechanical compaction may result in more intimate binding between the $TiO_2$ particles and the cementitious materials than that in Spray A, the Spray AB sample was selected to undergo the abrasion test. For comparison, a $TiO_2$-intermixed sample was also used for the same test. No obvious changes in NO

photodegradation were observed for the $TiO_2$-intermixed sample before and after the abrasion. In contrast, the abrasion action significantly affected the Spray AB sample. After 100 times abrasion action, the NO removal rate was reduced from 6.16 mg $h^{-1}$ $m^{-2}$ to 4.78 mg $h^{-1}$ $m^{-2}$. However, it is noteworthy that even after 100 times of abrasion, the NO removal rate of the Spray AB sample was still higher than that of the 5%$TiO_2$-intermixed sample (Fig. 5).

Two reasons may possibly explain the observed high NO removal ability and a relatively high weathering tolerance of the Spray AB samples. First, the prepared surface layers were rich in different sizes of pores. These pores could accommodate a large part of sprayed-on $TiO_2$ particles. Apparently, the $TiO_2$ particles nestling in the pores were well protected from the abrasion action. Fig. 6 shows the surface morphology of Spray AB and 5%$TiO_2$-intermixed samples after undergoing 100 times of abrasion. It clearly demonstrated the influence of the harsh abrasion on the surface layers and as a result of the abrasion, some grooves were left on the surface. It can be seen that a major fraction of white $TiO_2$ particles safely survived the harsh abrasion action, and remained in the pores. As for the 5%$TiO_2$-intermixed surface layer, no obvious white $TiO_2$ particles can be seen on the surface of the sample, indirectly indicating a lower photocatalytic activity. Another possible explanation may be due to the fact that as the hydration reaction progressed, most of the sprayed $TiO_2$ particles were successively and closely bounded to the hydration products. This scenario was likely to happen because the $TiO_2$ particles were sprayed on the surface of the samples immediately after they were prepared.

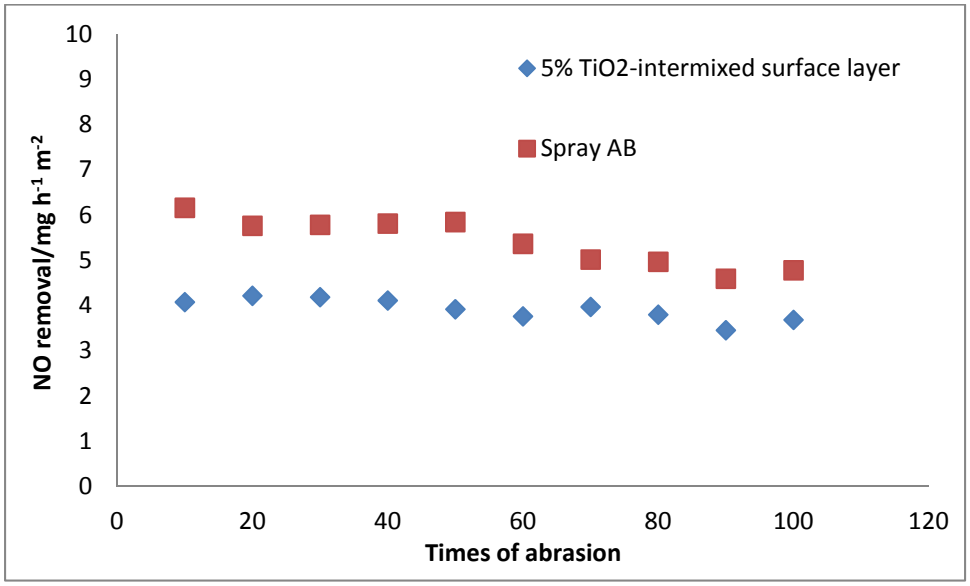


**Figure 5. Photocatalytic NO removal rate of different samples as a function of times of abrasion**

**Figure 6. Photograph of Spray AB (left) and 5%$TiO_2$ intermixed surface layer (right) undergone 100 times abrasion**

## 4. CONCLUSION

In the present work, an effective way to incorporate nano-$TiO_2$ in photocatalytic cementitious materials has been demonstrated. The results presented above reveal that this spraying method is promising and attractive mainly based on the following four reasons: a) The NO photocatalytic removal efficiency is relatively high; b) The sprayed $TiO_2$ particles on the surface display a satisfactory weathering resistance; c) This technique is easy to apply; d) This method brings down the cost.


## ACKNOWLEDGMENTS

The authors wish to thank Environment and Conservation Fund and Woo Wheelock Green Fund and The Hong Kong Polytechnic University for funding support.

## REFERENCES


Chen, J., and Poon, C. S. (2009). "Photocatalytic construction and building materials: from fundamentals to application." *Build Environ*, 44, 1899-1906.

Chen, J., Kou, S. C., and Poon, C. S. (2011) "Photocatalytic cement-based materials: comparison of nitrogen oxides and toluene removal potentials and evaluation of self-cleaning performance." *Build Environ*, 46, 1827-1833.

Diamanti, M. V., Ormellese, M., and Pedeferri, M. (2008). "Characterization of photocatalytic and superhydrophilic properties of mortars containing titanium dioxide." *Cement Concrete Res*, 38, 1349-1353.

Fujishima, A., Rao, T. N., and Tryk, D. A. (2000). "Titanium dioxide photocatalysis." *J Photoch Photobio C*, 1, 1-21.

Fujishima, A., Zhang, X. T., and Trylc, D. A. (2008). "$TiO_2$ photocatalysis and related surface phenomena." *Surf Sci Rep*, 63, 515-582.

Guo, M. Z., Ling, T. C., and Poon, C. S. (2012a). "$TiO_2$-based self-compacting glass mortar: Comparison of photocatalytic nitrogen oxide removal and bacteria inactivation." *Build Environ*, 53, 1-6.

Guo, M. Z., Ling, T. C., and Poon, C. S. (2012b). "Nano-TiO2-based architectural mortar for NO removal and bacteria inactivation: Influence of coating and weathering conditions." *Cement Concrete Comp*, http://dx.doi.org/10.1016/j.cemconcomp.2012.08.006.

Henderson, M. A. (2011). "A surface science perspective on $TiO_2$ photocatalysis." *Surf Sci Rep*, 66, 185-297.

Poon, C. S., and Cheung, E. (2007). "NO removal efficiency of photocatalytic paving blocks prepared with recycled materials." *Constr Build Mater*, 21, 1746-1753.

Rachel, A., Subrahmanyam, M., and Boule, P. (2002). "Comparision of photocatalytic efficiencies of $TiO_2$ in suspended and immobilised form for the photocatalytic degradation of nitrobenzenesulfonic acids." *Appl Catal B Environ*, 37 (4), 301-308.

Rout, B., Plassais, A., Olive, F., Guillot, L., and Bonafous, L. (2009). "$TiO_2$-containing cement pastes and mortars: measurements of the photocatalytic efficiency using a rhodamine B-based colourimetric test." *Solar Energy*, 83, 1794-1801.

Ramirez, A. M., Demeestere, K., De Belie, N., Mantyla, T., and Levanen, E. (2010). "Titanium dioxide coated cementitious materials for air purifying purposes: preparation, characterization and toluene removal potential." *Build Environ*, 45, 832-838.